

Live Firing and 3D Numerical Investigation of Base Bleed Exit Configuration Impact on Projectile Drag

M. Aziz, A. Ibrahim, A. Riad and M. Y. M. Ahmed*

Military Technical College, Cairo, Egypt

The manuscript was received on 4 September 2021 and was accepted after revision for publication as research paper on 15 May 2022.

Abstract:

Base bleed, in which gases are discharged at the base of projectile, is confirmed to be an effective drag reduction technique. It is believed that the design of base exit can impact the pattern of gas bleeding and, hence, the level of drag reduction. The present study is aimed to address this dependence that was not clarified in previous studies by examining the reduction in drag acting on a projectile with two different base bleed exit configurations. The first configuration includes a central circular orifice while the other is modified to include a smaller central circular orifice and four annular slots with equivalent total area. Numerical simulations on 3-D computational domain have been conducted to estimate drag and to explore the base flowfield for each configuration. The computational results at different Mach numbers have been compared with the mean drag based on range shooting for projectiles with both base configurations. In addition, different simulations have been performed to predict the real pattern of bleeding through the modified configuration based on the comparison with firing data at different Mach numbers.

Keywords:

aerodynamics, base bleed, CFD, drag reduction, live firing, range extension

1 Introduction

Range extension of artillery munitions has been (and still is) the prime objective for ballisticians. Currently, range extension can be achieved in many ways including increasing muzzle velocity, using an assistant rocket, using sub-caliber projectile, or reducing drag. The latter method is attained either by the forebody pressure drag reduction or base drag reduction which in turn is achieved by boat-tailing or increasing the base pressure [1]. Basically, the free shear layer at the projectile base corner engulfs a region of low-pressure recirculating flow known as the primary recirculation region (PRR). Hence, base pressure is reduced. There are two approaches to increase the

* Corresponding author: Aerospace Engineering Department, Military Technical College, Cairo, Egypt. Phone: +2-022 80 26 21, E-mail: mahmoud.yehia@mtc.edu.eg. ORCID 0000-0002-1991-0317.

pressure at the projectile base, namely passive and active devices. Passive devices such as base ventilated cavities and multistep base configurations were found to yield 10-20 % and 25-50 % reduction in base drag, respectively [2-5]. The stream wise slotted cavity is another passive device [6] that was found to yield a drag reduction; though insignificant due to the endured viscous losses. Active devices in base drag reduction include external burning [7-10] and base bleed. Nonetheless, using boattailing along with base bleed unit is the most common method of increasing base pressure [11, 12].

Base bleed device incorporates a propellant grain (of various shapes [13]) that acts as a gas generator. Upon burning, the gas generated acts to increase the density at the base area. In addition, the PRR shifts downstream due to the injected gases that also create a secondary recirculation region (SRR). In effect, the base pressure behind the projectile increases and the total projectile drag is eventually reduced with the penalty of increased dispersion due to inconsistent unit function [14]. The flows past a projectile with/without base bleed are schematically compared in Fig. 1.

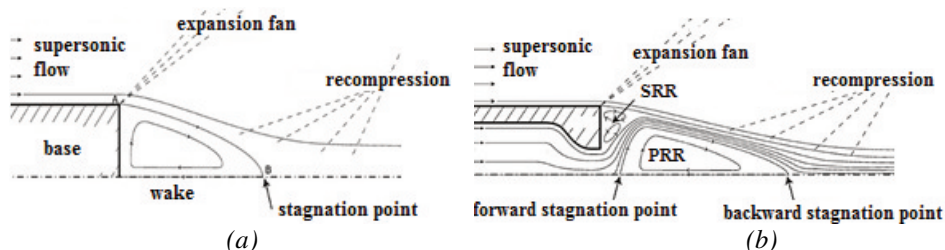


Fig. 1 Illustration of flow past a supersonic projectile with (a) blunt base and (b) base bleed [15]

The aspects of drag reduction by base bleed have attracted researchers for decades. It is widely agreed that the key parameter that controls the degree of drag reduction using base bleed is the rate of gas bleeding [16, 17] which is dependent on the burning rate of base bleed grain and pressure difference across the bleed exit [18, 19]. The set of flow visualization experiments by Dutton et al. [16, 19-22] provided good understanding of base flow features with central base bleed. Recent studies on base bleed focused on finer details of base bleed operation such as muzzle exit transients [23-25], fracture mechanisms of base bleed grain [26, 27], post-combustion of base bleed unit [28], impact of projectile spin [29], and implementing advanced numerical simulation techniques [30].

Drag reduction via base bleed is clearly a fluid dynamics problem. Karsten [31] pointed out that modeling the base bleed simply as a fluid injector yields fairly accurate prediction. Therefore, it has been believed that not only gas bleeding rate but also bleeding pattern may control the drag reduction level. Cavalleri and Posey [32] conducted a numerical simulation study to compare central orifice and annular (edge) slots in base drag reduction. Both axial and inclined edge injections were examined; the annular edge injection was found more effective than the central injection. In their numerical simulation study, Kubberud et al. [33] pointed out that even minor changes in the bleed exit configuration have an impact on drag reduction. Yu et al. [34, 35] conducted a set of numerical simulation studies to compare the annular edge slots and circular central orifice (keeping the same overall exit area) on the base pressure at different injection rate values at Mach 2 free stream. Yu et al. confirmed the findings in [34] as they concluded that the annular slots over-performed the central orifice. They

also concluded that the closer the slots to the base edge, the higher the base pressure. Finally, Zhou et al. [36] through their numerical simulation study confirmed the findings of Yu et al. [34] that while the base pressure reaches a peak value at an optimum injection rate using the central orifice, the base pressure increases monotonically with the injection rate using annular slots.

Despite the good coverage of the studies stated above, a number of gaps can be addressed. Firstly, the previous studies on the base bleed configuration relied on numerical simulations solely (e.g. [37]) or they were validated against previous wind tunnel testing as in [19, 25, 38] or firing tables as in [39]. In addition, (axisymmetric) 2D computational domains were used [25] even with annular exits [32] implying full annular exits which may not be practically valid. Secondly, the use of live firing to assess the numerical simulation results was not presented in the previous literature. Thirdly, the impact of the simultaneous use of central orifice and edge annular slots was not investigated before. Finally, an investigation whether the burn pattern of the base bleed grain impacts the unit performance was not addressed in the previous studies.

The present research is a side-by-side firing-simulation study that was carried out on one type of base bleed projectiles with a threefold objective. Firstly, the objective was to address the impact of bleed exit configuration on the drag acting on the projectile. Two configurations are compared, the first is a single central orifice whereas the other one is annular slots along with a smaller central orifice with the same gas flow rate as the first one. This was conducted via a 3D numerical simulation to understand the physics of the base flow for each configuration. Secondly, to assess the simulation results, a set of projectiles for each configuration was manufactured and fired. The total drag coefficient for each round was estimated based on the real flight data. The computed total drag coefficients were compared with experimental counterparts at different Mach numbers and the differences were addressed and explained. On the other hand, the impact of bleed grain regression pattern on projectile total drag was addressed based on contrasting simulation and live firing results. The use of total projectile drag coefficient based on live firing results has been widely adopted to assess both the quality of simulations and the impact of base bleed [5, 15, 17, 29, 35, 40].

In the following section, details of the case study projectiles are presented. Next, the methodology of the study is explained in details. The results are then discussed and the main conclusions and recommendations conclude the present paper.

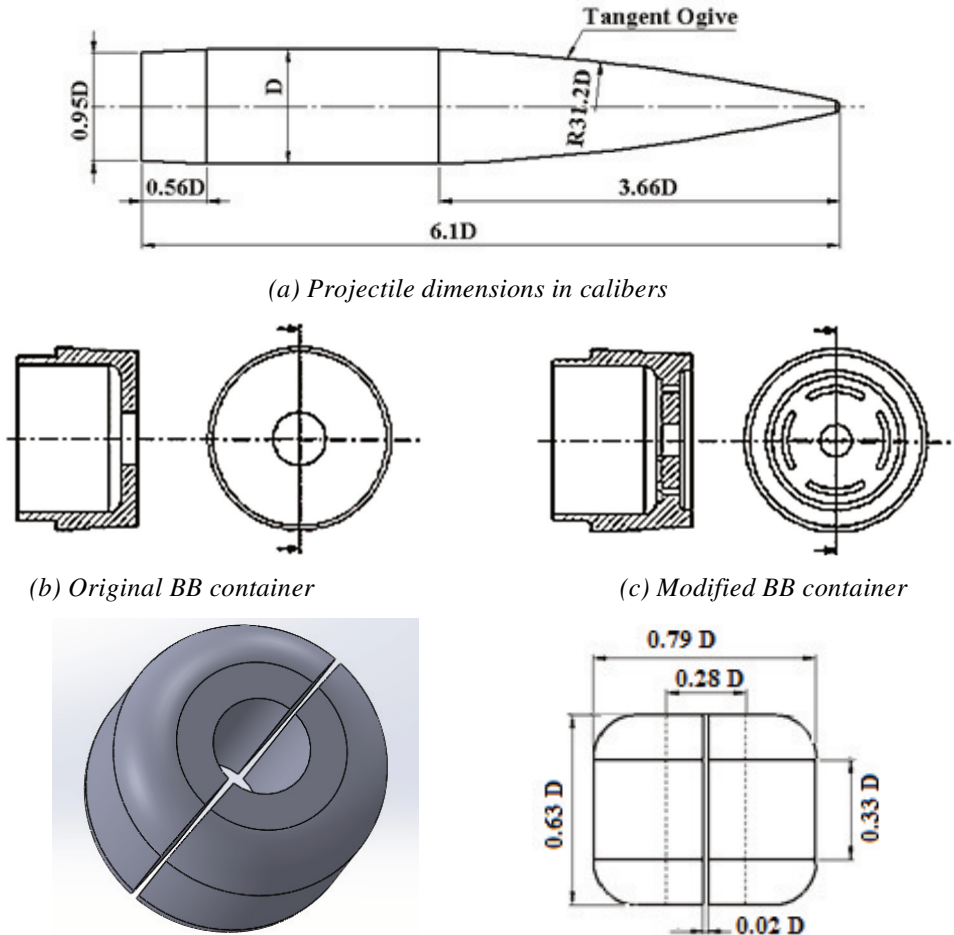
2 Case Study and Methodology

2.1 Case Study

A projectile with two different base bleed unit exit configurations was studied; its dimensions in terms of caliber are shown in Fig. 2a. The original and modified exit configurations are shown in Figs 2b and 2c, respectively. The 0.285D central orifice in the original configuration was replaced with a smaller one (for grain ignition purposes) along with four symmetric annular orifices. The total area of bleeding exits was maintained; the central orifice and annular slots in the modified configuration had the area ratio of 2:3.

The base bleed grains in both designs are the same; a slotted tubular grain was burned from the inner surface out. The configuration and geometric dimensions of the grain are shown in Fig. 2d. During production, the grain was placed inside the allocated cavity at the rear of the projectile and the container is then screw-fitted into projectile.

In operation, the grain was ignited by the projectile charge soon as the projectile had left the muzzle. The ratio of the mass of the projectile to the mass of the base bleed grain was about (35.7:1). The gain was burned out in 30 s yielding a low-subsonic bleeding of gases out of the unit with an average flow rate of 0.045 kg/s.



(d) Base bleed grain configuration and dimensions in calibers

Fig. 2 Geometric details of the case study model

2.2 Live Firing Experiments

The projectiles with original and modified base bleed units were especially manufactured for the purpose of the present research. Two sets of original and modified projectiles were fired from the same gun including five and seven rounds, respectively. The instantaneous projectile location relative to the gun during flight was captured using a mono-pulse Doppler antenna. Temporal variation of trajectory parameters including range, altitude, velocity was calculated by analyzing the output of tracking radar and the total drag coefficient was then estimated [41]. All firings were conducted at a fixed elevation angle namely, 45 degrees.

2.3 Numerical Simulations Setup

The drag on projectile with two different bleed exit configurations at different Mach values and zero incidence was estimated via computational simulations. Since the modified projectile was not axisymmetric, a computational domain representing one-eighth of full 3D domain was adopted, Fig. 3.

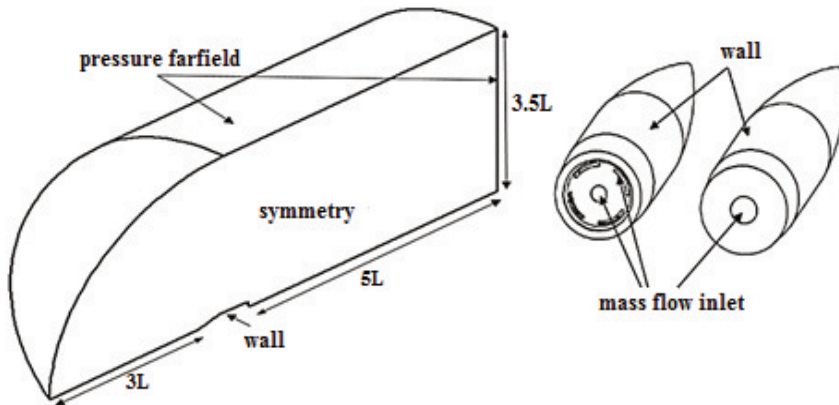


Fig. 3 Illustration of computational domain and boundary definition

Domain extents were 3, 3.5, and 5 times the projectile length in the upstream, lateral and downstream directions, respectively. Boundary definitions were set as shown in Fig. 3. At the pressure farfield boundary, static pressure, temperature, and Mach number corresponding to real flight conditions [42] were defined. At the base bleed exit, velocity inlet was defined corresponding to gas flow rate. The lateral side planes were defined as symmetric while adiabatic no slip conditions were defined to the solid projectile surfaces. A multi-block structured grid was constructed and its resolution was enhanced at the areas of interest, Fig. 4.

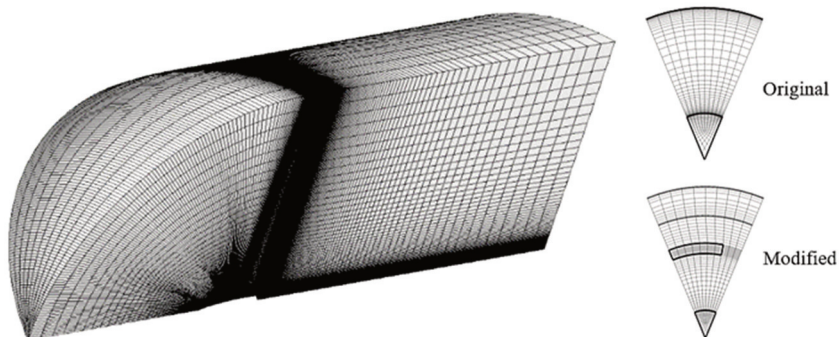


Fig. 4 Structured 3-D grid (one-eighth domain)

The density-based solver with a second-order discretization scheme were adopted in solving steady RANS equations. The freestream air flow was treated as ideal gas whereas the bleeding gas was defined with chemical reaction enabled [43]. A commercial CFD tool was utilized [44]. Two-equation turbulence models have been successfully used in similar simulations; K-epsilon model was implemented in [37, 45]

whereas K- ω model was used in [40, 46]. In the present work, the K- ϵ with Realizable Enhanced Wall Treatment turbulent model was used.

A grid sensitivity study was conducted on the original projectile with free stream conditions corresponding to Mach 1.5 at standard sea level atmosphere. Grids with different resolutions were constructed and projectile drag coefficient with active and inert base bleed was adopted as a measure of solution grid-independence. Fig. 5 shows the dependence of the projectile drag coefficient on the grid cell counts, N , normalized by that of the coarse one, NG . A grid with 714 500 cells (shown in solid markers) was chosen as no significant improvement was achieved with further cell count increase.

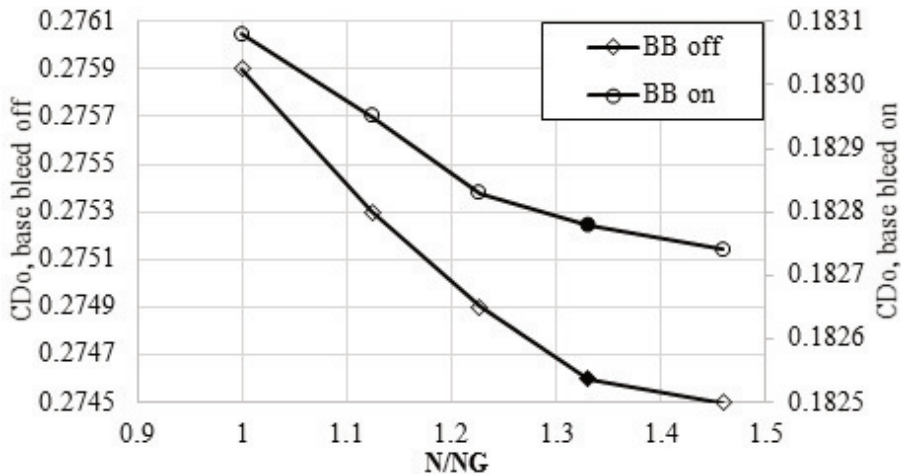


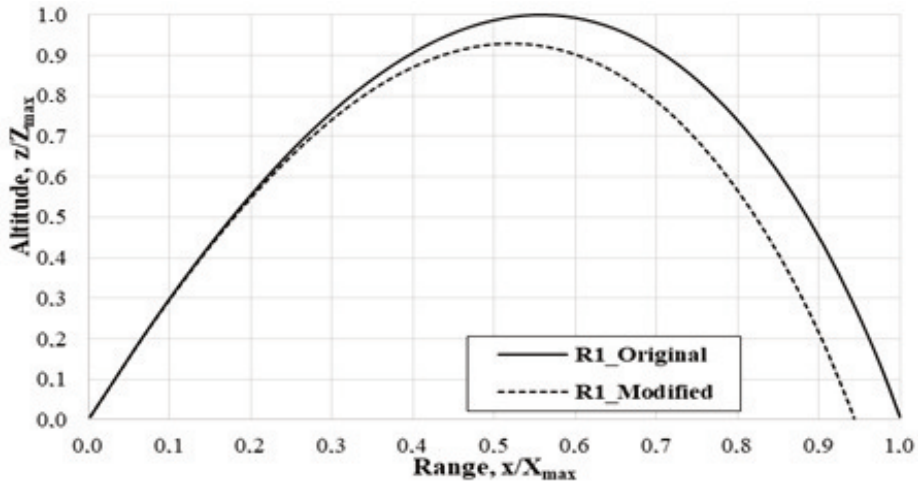
Fig. 4 Grid independence check results

3 Results and Discussions

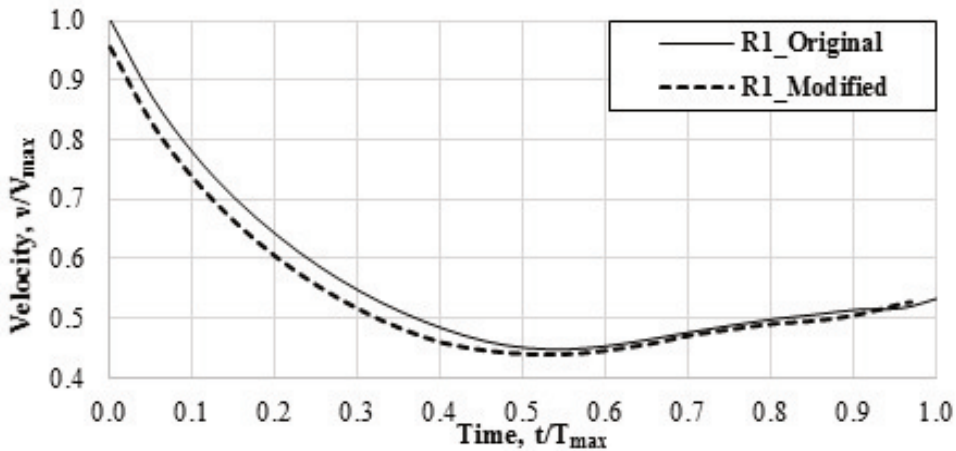
3.1 Results of the Live Firing for Projectile with both Original and Modified Bleed Exits

Five rounds for the original design and seven rounds for the modified one are fired. A sample output for live firing of projectiles with original and modified base bleed exit configurations is displayed in Fig. 6. The data are normalized with respect to those of the original round. The output data are manipulated further to estimate the variation of total drag coefficient with flight Mach number. The data for original rounds were reported in [47]; for the sake of completeness, these data are presented here along with those for the modified rounds.

The drag behavior for both original and modified rounds is better illustrated in Fig. 7a and 7b, respectively. For the sake of more comprehensible illustration, the Mach axis is split into two separate ranges; 1.2: 1.4 and 1.5: 1.8. To illustrate the impact of bleed exit configuration on the total projectile drag, Fig. 7c compares the mean drag coefficients for both designs.



(a) Altitude versus range



(b) Velocity versus time

Fig. 5 Sample output data from live firing of original and modified projectiles.

It can be inferred that the modified bleed exit yields a drag rise of about 0.3 % to 8 % over the range of Mach numbers greater than 1.2. It is also interesting to indicate that the modified design yields a lower drag at the lower limit of Mach that takes place near the summit point of projectile trajectory. An explanation for this behavior, which contradicts the finding of Yu et al. [34], is attempted shortly based on numerical simulation findings.

3.2 Comparison of Simulation with Live Firing Results for Both Original and Modified Projectiles

Tab. 1 lists the values of the total drag coefficient obtained from live firing and their computational counterparts for the original and modified projectiles.

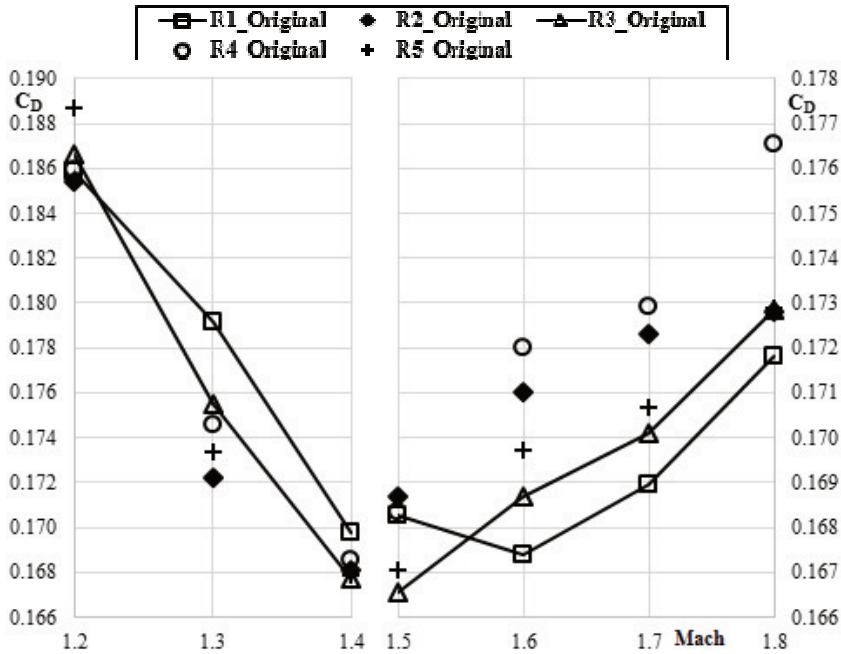


Fig. 7(a) Total drag coefficients versus Mach numbers for the original rounds [47]

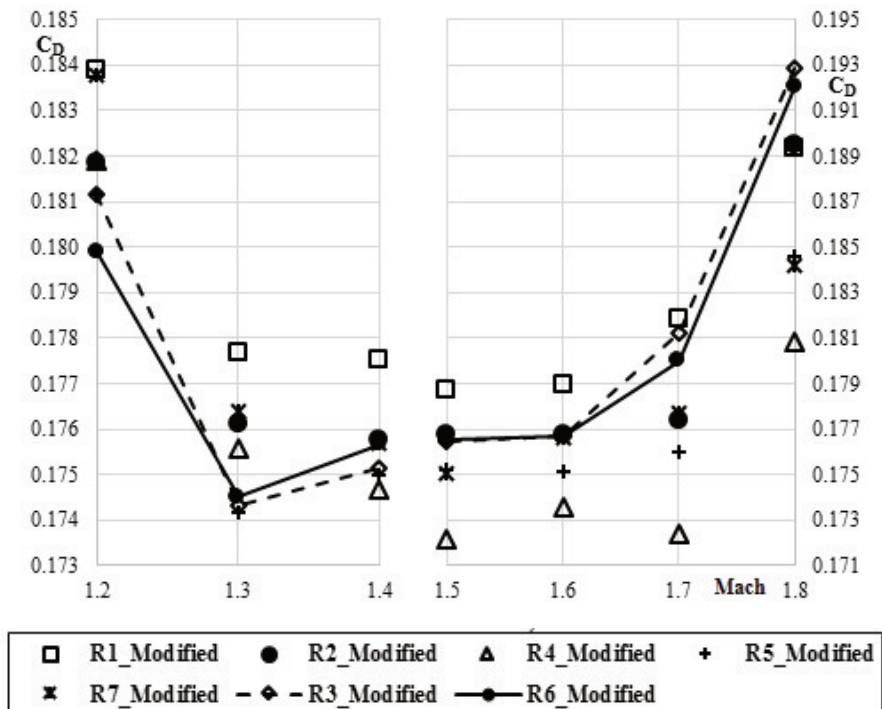
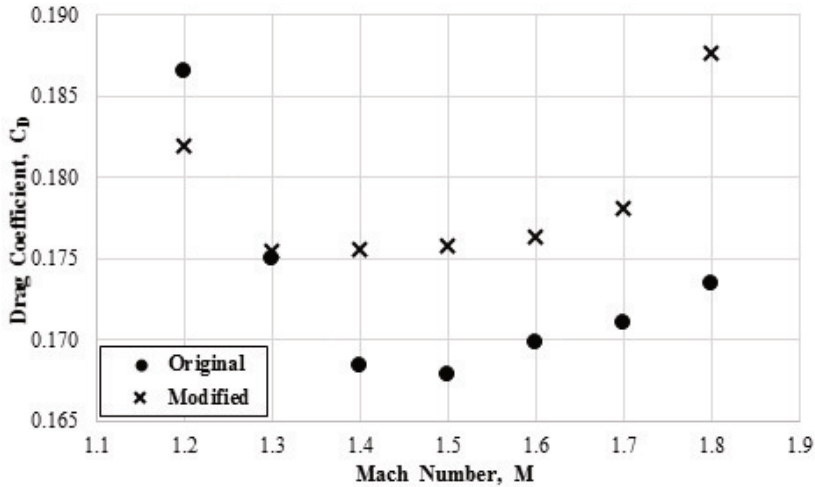


Fig. 7(b) Total drag coefficients versus Mach numbers for the modified rounds



(c) Means of total drag coefficient for both designs

Fig. 6 Live Firing data for total drag coefficients of the original and modified rounds

Tab. 1 Drag coefficients for original and modified projectiles based on live firing and simulation results

Mach	Original design [47]			Modified design		
	Live firing (Mean value)	CFD	Difference [%]	Live firing (Mean value)	CFD	Difference [%]
1.2	0.1865	0.1819	-2.46	0.1819	0.1687	-7.28
1.3	0.1750	0.1736	-0.80	0.1755	0.1656	-5.65
1.4	0.1684	0.1714	1.78	0.1756	0.1633	-7.06
1.5	0.1678	0.1695	1.01	0.1758	0.1613	-8.28
1.6	0.1698	0.1672	-1.53	0.1763	0.1589	-9.86
1.7	0.1710	0.1663	-2.75	0.1781	0.1592	-10.61
1.8	0.1734	0.1720	-0.81	0.1876	0.1599	-14.77

The deviation between the computational and experimental values for the original design does not exceed 2.75 %. On the other hand, it is clearly evident that the numerical simulation underestimates the drag at all Mach values for the modified design. Moreover, the deviation seems to increase almost monotonically with freestream Mach number. An explanation for this deviation is attempted below.

It is important first to recall that for the simulation of the modified design, the flow of gases is evenly distributed between the central orifice and the annular slots on an area basis. Since the total exit area is divided between central orifice and annular slot by the ratio 2:3, respectively, 60 % of the flow is imposed to exit through the annular slot in the numerical simulation. Hence, the deviations in Tab. 2 may be explained based on a hypothesis that the pattern of mass flow imposed by the simulation differs from the pattern taking place in real flight. Therefore, to test this hypothesis and to better understand the real pattern of gas bleeding, seven numerical simulation cases are developed (case#A to case#G) in which the percent of bleeding gases flowing through the central orifice varies from 40 % to 100 % of the total flow, respectively, with equal

intermediate steps of 10 %. For all seven cases, the same free stream flow conditions and flight speeds are defined according to the corresponding real flight altitudes based on firing results.

Fig. 7 illustrates the drag coefficients results for every tested bleeding ratio at each Mach number. For the sake of comparison, the mean values of live firing measurements of drag coefficients for the modified projectile at the corresponding Mach numbers are presented in the same figure.

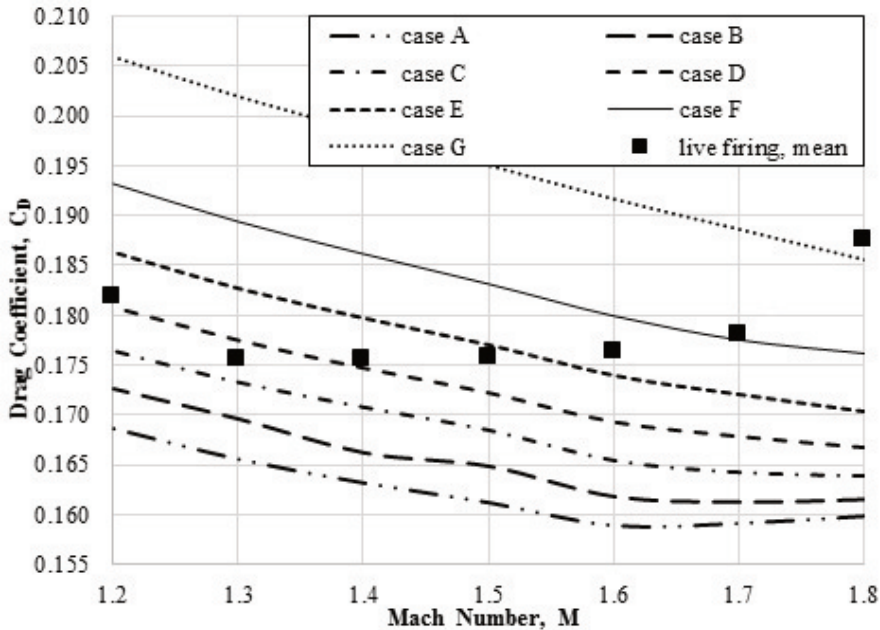


Fig. 7 Firing and simulation drag coefficients for modified projectile with different bleeding ratio for orifice and slots versus Mach number

By examining the simulation results, cases #A to #G, it is clear that the drag is maximum if all gases are made to bleed from the small central orifice only. The drag on the projectile decreases monotonically as the ratio of gases bleeding through the annular slots increases. This drop in drag is more pronounced at lower flow rates through slots and becomes less significant at higher slot flow rates. This drag behavior is evident for all values of Mach number. It can be thus confirmed that the annular slots bleeding is more effective in reducing the drag than that of the central orifice. Consequently, the modified projectile (with both central orifice and annular slots) should have experienced less drag during flight than the original one (with central orifice only). This contradicts the firing results shown in Fig. 7.

More interestingly, by contrasting the simulation results with the live firing data in Fig. 7, the variation of gas bleeding pattern with flight Mach number in the modified design can be addressed as follows. At the lower Mach limit, the simulation assumes that about 70 % of gases exit through the central orifice (case #D). At the upper Mach limit, the simulation results assume that 100 % of bleeding gases exit from the central orifice (case #G). At the intermediate Mach values, the percentage of central orifice gas bleeding increases from 70 % to 100 %.

The unexpected trend of the drag in live firing can be explained by recalling that the base bleed grain burns internally. At the beginning of the flight (at the upper Mach limit), combustion gases tend to flow entirely through the central orifice as the “nearest” exit (consistent with simulation case #G). As flight time passes, the flight Mach number drops while the grain inner port expands to such an extent that a small percentage of gases starts to exit the annular slots. By the end of the grain burn time, the flight Mach drops to its lower limit while the grain is almost burnt out increasing the percentage of gases bleeding through slots to 30 % (consistent with simulation case #D).

If an end-burning (cigarette) grain is used instead of the internally-burning grain, a different pattern of bleeding is expected. It can be also predicted that a base unit with the annular slot only (no central orifice) would yield a lower drag on the projectile. In such case, all gases would have to flow through slots at all times (i.e., for all Mach values) yielding a lower drag over the entire bleeding time. To confirm this hypothesis, a final set of simulations is made in which all gases are made to bleed from the annular orifices only. The resulting drag coefficient is compared with the corresponding mean of experimental measurements in Fig. 8.

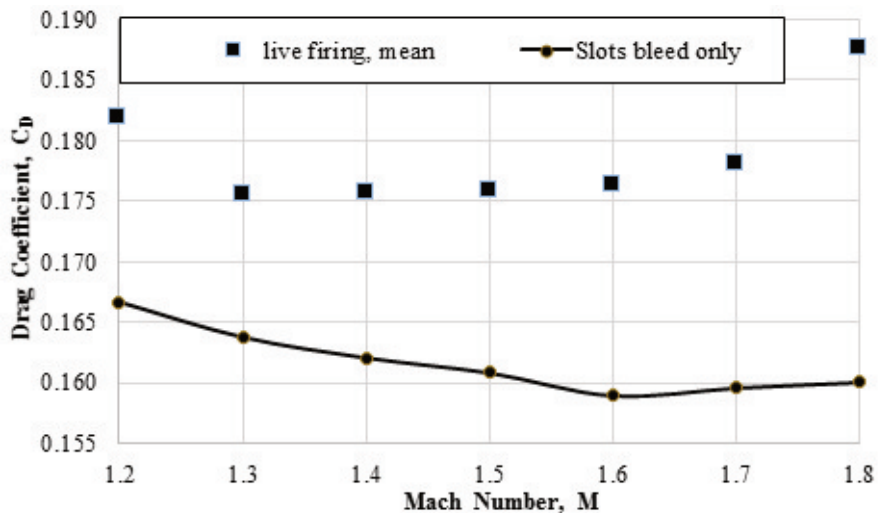


Fig. 8 Firing and simulation drag coefficients for modified projectile with slots bleeding only versus Mach number

Clearly, the drag on the projectile is minimized if all gases are made to bleed from the annular orifice. This conclusion is consistent with the findings of Yu et al. [34]. If this burn pattern is sought, the central orifice should be eliminated and an alternative ignition technique that does not demand a central orifice may be needed.

Finally, it is interesting to explore the base flowfield structure based on the simulation results. Fig. 9 shows the pressure contours and streamlines in the base region at Mach number 1.8 for different bleeding ratios: case #A; the orifice bleeding ratio 40 % and case #G; the orifice bleeding ratio 100 %. For the sake of comparison, the base flowfield structure associated with the inert projectile is also shown.

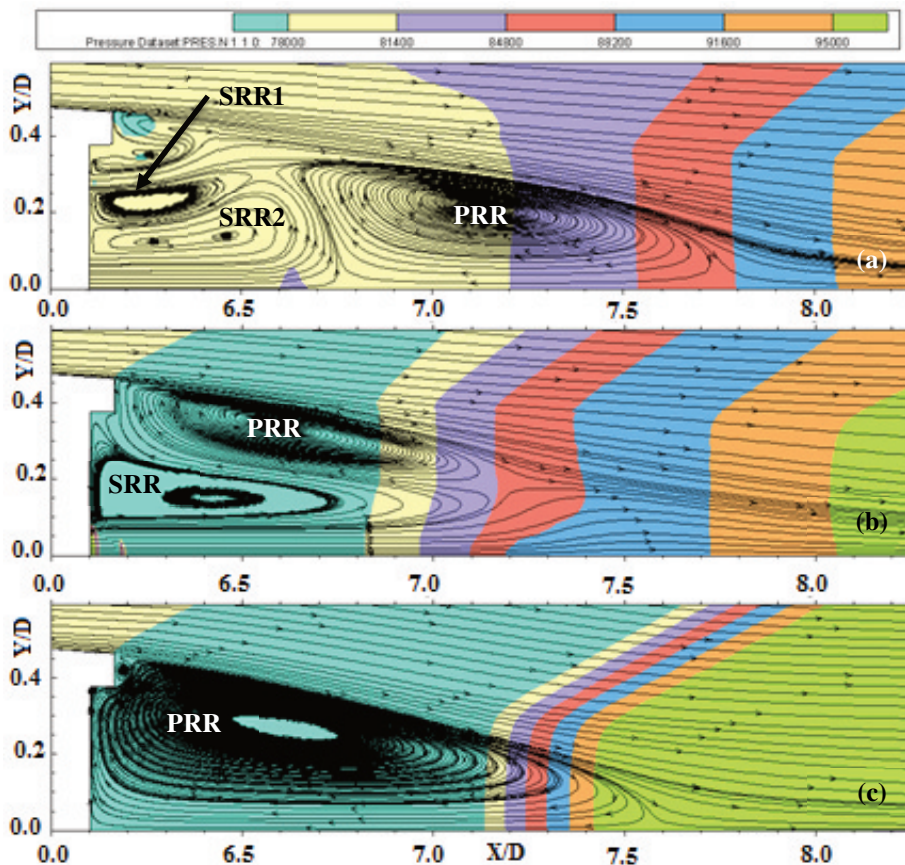


Fig. 9 Pressure contour and streamlines for base region at Mach 1.8 for (a) case #A; 40 % orifice bleeding, (b) case #G; 100 % orifice bleeding, and (c) inert projectile

The large primary recirculation region (PRR) is evident in the inert projectile case, Fig. 9c. For case #A Fig. 9a, gases bleed from both orifice and slots. This forces the primary recirculation region (PRR) to move further downstream. Two other smaller (weaker) secondary recirculation regions (SRR1, SRR2) are created between the orifice and slot flows. In effect, the base area is exposed to a flow with a relatively high density (and pressure).

For case #G, Fig. 9b, all gases bleed from the orifice only. Thus, the gases velocity increases compared to that in case #A. As a consequence, the primary recirculation region is changed from an ellipsoid shape (as in case of the inert projectile, Fig. 9c, to a toroidal one and a reversal in recirculation direction takes place. A secondary large recirculation region (SRR) is created in the zone engulfed by the shear layer (SL) and (PRR). Eventually, air density (and pressure) are lower than those for case #G. This yields a lower base (and total) drag for case #A than those in case #G.

4 Conclusions and Recommendations

Live firing and 3D numerical simulations for two different bleeding exit shapes for a projectile with live base bleed are discussed in this paper. The objective was to assess and understand the impact of gas exit configuration on total projectile drag, to assess the simulation results via comparing them with the live firing results, and to address the impact of the base bleed grain burn pattern on the unit operation.

The original base configuration had one central orifice, the computation results and the firing measurements of the drag coefficient at different Mach numbers were consistent with maximum deviation of 2.75 %. The modified base configuration had a smaller central orifice and four annular slots near the base edge. The firing drag coefficient measurements of the modified base were matched with a remarkable accuracy if the ratio of flow rates through orifice and slots are accurately predicted based on the pattern of base bleed grain regression. This pattern resulted in a time-dependent variation of mass flow rates through orifice and slots. This indicates that the pattern of base bleed regression has an impact on base bleed unit drag reduction benefits. In addition, the flow field structure at the base region is explored for both configurations and compared with that of inert projectile.

It is concluded that the drag on the projectile can be minimized if all bleeding gases flow through the annular exits. In the present case, a central orifice was imposed as a design constraint to allow for base bleed grain ignition. For future development, alternative ignition technique is sought in which the central orifice is completely replaced.

References

- [1] IBRAHIM, A. and A. FILIPPONE. Effect of Porosity Strength on Drag Reduction of a Transonic Projectile. *Journal of Aircraft*, 2007, **44**, pp. 310-316. DOI 10.2514/1.23613.
- [2] VISWANATH, P.R. Passive Devices for Axisymmetric Base Drag Reduction at Transonic Speeds. *Journal of Aircraft*, 1988, **25**(3), pp. 258-262. DOI 10.2514/3.45586.
- [3] VISWANATH, P.R. and S.R. PATIL. Effectiveness of Passive Devices for Axisymmetric Base Drag Reduction at Mach 2. *Journal of Spacecraft and Rockets*, 1990, **27**(3), pp. 688-691. DOI 10.2514/3.26130.
- [4] VISWANATH, P.R. Flow Management Techniques for Base and Afterbody Drag Reduction. *Progress in Aerospace Science*, 1996, **32**, pp. 79-129. DOI 10.1016/0376-0421(95)00003-8.
- [5] VISWANATH, P.R. Drag Reduction of Afterbodies by Controlled Separated Flow. *AIAA Journal*, 2001, **39**(1), pp. 73-78. DOI 10.2514/2.1272.
- [6] IBRAHIM, A. and A. FILIPPONE. Effect of Streamwise Slots on the Drag of a Transonic Projectile. *Journal of Aircraft*, 2007, **44**, pp. 1865-1876. DOI 10.2514/1.30439.
- [7] SMITHEY, W., M. NABER, G. CASWELL and A.E. FUHS. External Burning Assisted Projectile- Theory and Experiment. In: *9th Propulsion Conference*. Las Vegas: American Institute of Aeronautics and Astronautics and Society of Automotive Engineers, 1973. DOI 10.2514/6.1973-1193.

-
- [8] SMITHEY, W. and A.E. FUHS. Projectile Thrust-Drag Optimization with External Burning. *Journal of Aircraft*, 1977, **14**(11), pp. 1025-1026. DOI 10.2514/3.58886.
- [9] SCHETZ, J., F. BILLIG and S. FAVIN. Analysis of Base Drag Reduction by Base and/or External Burning. *AIAA Journal*, 1981, **19**(9), pp. 1145-1150. DOI 10.2514/3.60053.
- [10] MEHTA, G.K. and W.C. STRAHLE. Analysis of Axially Symmetric External Burning Propulsion for Bluff-Base Bodies, *AIAA Journal*, 1979, **17**(3), pp. 269-270. DOI 10.2514/3.61111.
- [11] KORKEGI, R.H. and L.M. FREEMAN. Aft-Body Drag Reduction by Combined Boat-Tailing and Base Blowing at $M = 3$. *AIAA Journal*, 1976, **14**(8), pp. 1143-1145. DOI 10.2514/3.7206.
- [12] ANDERSON, K., N.E. GUNNERS and R. HELLGREN. Swedish Base Bleed-Increasing the Range of Artillery Projectiles through Base Flow. *Propellants and Explosives*, 1976, **1**, pp. 69-73. DOI 10.1002/prop.19760010402.
- [13] ZAKI, A., M.S. ABDEL-KADER and H. YAKOUT. Performance of Artillery Projectiles with Base Bleed Unit. In: *8th International Conference on Aerospace Sciences & Aviation Technology*. Cairo: Military Technical College, 1999, pp. 71-84. DOI 10.21608/asat.1999.24873.
- [14] ZHANG, L., Y.-H. ZHOU, Y.-G. YU and W. ZHAO. Study on Firing Range Dispersion of Base Bleed Projectile Caused by Inconsistent Base Bleed Unit Working. In: *25th International Symposium on Ballistics*. Beijing: China Ordnance Society, 2010, pp. 258-285.
- [15] KADIC, S.S., B. ZECEVIC, J. TERZIC and A. CATOVIC. Influence of Local Atmosphere Characteristics to Range of 155 mm M864 Projectile. In: *15th Seminar of New Trends in Research of Energetic Materials*. Pardubice: University of Pardubice, 2012, pp. 790-799. ISBN 978-80-7395-480-2.
- [16] MATHUR, T. and J.C. DUTTON. Velocity and Turbulence Measurements in a Supersonic Base Flow with Mass Bleed. *AIAA Journal*, 1996, **34**(6), pp. 1153-1159. DOI 10.2514/3.13206.
- [17] SAHU, J. and C.J. NIETUBICZ. Navier-Stokes Computations of Projectile Base Flow with and without Mass Injection. *AIAA Journal*, 1985, **23**(9), pp. 1348-1355. DOI 10.2514/3.9091.
- [18] CLAYDEN, W.A. and J.E. BOWMAN. Cylindrical Afterbodies at M Sub Infinity Equals 2 with Hot Gas Ejection. *AIAA Journal*, 1968, **6**(12), pp. 2429-2431. DOI 10.2514/3.5009.
- [19] MATHUR, T. and J.C. DUTTON. Base-Bleed Experiments with a Cylindrical Afterbody in Supersonic Flow. *Journal of Spacecraft and Rockets*, 1996, **33**, pp. 30-37. DOI 10.2514/3.55703.
- [20] BOURDON, C.J. and J.C. DUTTON. Turbulence Structure of a Compressible Base Flow with a Central Bleed Jet. *Journal of Spacecraft and Rockets*, 2004, **41**(3), pp. 451-460. DOI 10.2514/1.10722.
- [21] KUEHNER, J.P. and J.C. DUTTON. Planar Fluorescence Imaging of a Supersonic Axisymmetric Base Flow with Mass Bleed. *AIAA Journal*, 2005, **43**(8), pp. 1767-1775. DOI 10.2514/1.13226.

- [22] KUEHNER, J.P., B.B. ANDERSON, J.G. FLITTNER and J.C. DUTTON. Characteristics of a Central Bleed Jet in Supersonic Axisymmetric Base Flow. *Journal of Spacecraft and Rockets*, 2007, **44**(2), pp. 347-353. DOI 10.2514/1.24838.
- [23] MA, L. and Y. YU. Coupling Characteristics of Combustion-Gas Flows Generated by Two Energetic Materials in Base Bleed Unit Under Rapid Depressurization. *Applied Thermal Engineering*, 2019, **148**, pp. 502-515. DOI 10.1016/j.applthermaleng.2018.11.071.
- [24] ZHOU, S. and Y. YU. Numerical Study of Initial Pressure in Unsteady Flow Field with Base Bleed. In: *31st International Symposium on Ballistics*. Hyderabad: DEStech Publications, 2019, pp. 1137-1148. ISBN 978-1-60595-610-7.
- [25] LEE, Y.K., H.D. KIM and S. RAGHUNATHAN. Optimization of Mass Bleed for Base-Drag Reduction. *AIAA Journal*, 2007, **45**(7), pp. 1472-1477. DOI 10.2514/1.23085.
- [26] WU, Z., QIAN, J. and G. NIU. Experimental Investigation of Compressive Mechanical Properties and Fracture Mechanics of AP-HTPB Base Bleed Grain. In: *30th International Symposium on Ballistics*, California: DEStech Publications, 2017, pp. 739-746. ISBN 978-1-60595-419-6.
- [27] WU, Z., G. NIU, J. QIAN and R. LIU. Study on Impact Compressive and Tensile Mechanical Properties of HTPB Composite Base Bleed Grain at Various Temperatures. In: *31st International Symposium on Ballistics*. Hyderabad: DEStech Publications, 2019, pp. 451-461. ISBN 978-1-60595-610-7.
- [28] XUE, X. and Y. YU. An Improvement of the Base Bleed Unit on Base Drag Reduction and Heat Energy Addition as well as Mass Addition. *Applied Thermal Engineering*, 2016, **109**, pp. 238-250. DOI 10.1016/j.applthermaleng.2016.08.072.
- [29] PÉREZ, F.N., F.J.S. VELASCO, J.R.G. CASCALES, R.A.O. MARTÍNEZ, A.L. BELCHÍ, D. MORATILLA, F. REY and A. LASO. On the Accuracy of RANS, DES and LES Turbulence Models for Predicting Drag Reduction with Base Bleed Technology. *Aerospace Science and Technology*, 2017, **67**, pp. 126-140. DOI 10.1016/j.ast.2017.03.031.
- [30] PÉREZ, F.N., J. SERNA, B.A. LOPEZ, F.J.S. VELASCO, J.R.G. CASCALES, F. REY, A. LASO, R.A.O. MARTÍNEZ, R. MUR, D. MORATILLA and R.A.G. UGARTE. Probase: A Software Application to Estimate Drag in Base Bleed Technology Units Using Large Eddy Simulations. In: *30th International Symposium on Ballistics*. California: DEStech Publications, 2017, pp. 373-383. ISBN 978-1-60595-419-6.
- [31] KARSTEN, P.A. Modeling Base Bleed as an Injector. In: *27th International Symposium on Ballistics*, Freiburg: DEStech Publications, 2013. ISBN 978-1-60595-106-4.
- [32] CAVALLERI, R.J. and S.A. POSEY. Effect of Injection Configuration on Base Drag Reduction. In: *26th AIAA Aerospace Sciences Meeting*. Reno: American Institute of Aeronautics and Astronautics, 1988. DOI 10.2514/6.1988-213.
- [33] KUBBERUD, N. and L.J. OYE. Extended Range of 155mm Projectile Using an Improved Base Bleed Unit. Simulation and Evaluation. In: *26th International Symposium on Ballistics*. Miami: DEStech Publications, 2011. ISBN 978-1-60595-052-1.

- [34] YU, W.J., Y.G. YU and B. NI. Numerical Simulation of Base Flow with Hot Base Bleed for Two Jet Models. *Defence Technology*, 2014, **10**. DOI 10.1016/j.dt.2014.06.010.
- [35] YU, W.J., Y.G. YU and B. NI. Numerical Simulation on Effects of Annular Jet in Base Flow of Base Bleed. *Chinese Journal of Energetic Materials*, 2014, **22**(3), pp. 318-324. DOI 10.3969/j.issn.1006-9941.2014.03.009.
- [36] ZHOU, C.F., X.S. WU and F. FENG. Effect of Base Bleed Type on Drag Reduction Performance in Supersonic Flow. *Acta Aeronautica et Astronautica Sinica*, 2015, **35**(8), pp. 2144-2155. DOI 10.7527/S1000-6893.2013.0488.
- [37] KAURINKOSKI, P. and A. HELLSTEN. Numerical Simulation of a Supersonic Base-Bleed Projectile with Improved Turbulence Modeling. *Journal of Spacecraft and Rockets*, 1998, **35**(5), pp. 606-611. DOI 10.2514/2.3392.
- [38] SAHU, J. and K.R. HEAVEY. Numerical Investigation of Supersonic Base Flow with Base Bleed. *Journal of Spacecraft and Rockets*, 1997, **34**(1), pp. 62-69. DOI 10.2514/2.3173.
- [39] DANBERG, J.E. and C.J. NIETUBICZ. Predicted Flight Performance of Base-Bleed Projectiles. *Journal of Spacecraft and Rockets*, 1992, **29**(3), pp. 366-372. DOI 10.2514/3.26360.
- [40] DALI, M.A. and S. JARAMAZ. Optimization of Artillery Projectiles Base Drag Reduction using Hot Base Flow. *Thermal Science*, 2019, **23**(1), pp. 353-364. DOI 10.2298/TSCI180413210D.
- [41] DUTTA, G.G., A. SINGHAL, A. KUSHARI and A.K. GHOSH. Estimation of Drag Coefficient from Radar-tracked Flight Data of a Cargo Shell. *Defence Science Journal*, 2008, **58**(3), pp. 377-389. DOI 10.2514/6.2006-6149.
- [42] ABOU-ELELA, H.A., A.Z. IBRAHIM, O.K. MAHMOUD and O.E. ABDEL-HAMID. Ballistic Analysis of a Projectile Provided with Base Bleed Unit. In: *15th International Conference on Aerospace Sciences & Aviation Technology*. Cairo: Military Technical College, 2013. DOI 10.21608/asat.2013.22270.
- [43] MARZOUK, O.A. and E.D. HUCKABY. A Comparative Study of Eight Finite-Rate Chemistry Kinetics for CO/H₂ Combustion. *Engineering Applications of Computational Fluid Mechanics*, 2010, **4**, pp. 331-356. DOI 10.1080/19942060.2010.11015322.
- [44] ANSYS FLUENT Theory Guide Release 14.5, ANSYS, 2013.
- [45] BELAIDOUNI, H., S. ŽIVKOVIĆ and M. SAMARDŽIĆ. Numerical Simulations in Obtaining Drag Reduction for Projectile with Base Bleed. *Scientific Technical Review*, 2016, **66**(2), pp. 36-42. DOI 10.5937/STR1602036B.
- [46] DE, A. and P. CHETTRI. Drag Reduction with Optimum Designing of a Base Bleed Projectile Using Computational Analysis. In: *Green Energy and Technology: Innovations in Sustainable Energy and Cleaner Environment*. Singapore: Springer, 2020, pp 23-46. ISBN 978-981-13-9011-1.
- [47] AZIZ, M.M., A.Z. IBRAHIM, M.Y.M. AHMED and A.M. RIAD. Multi-fidelity Drag Prediction for Base Bleed Projectile. In: *19th International Conference on Applied Mechanics and Mechanical Engineering (AMME-19)*. Cairo: Military Technical College, 2020, **973**, 012033. DOI 10.1088/1757-899X/973/1/012033.